COMPDYN 2015
5th ECCOMAS Thematic Conference on
Computational Methods in Structural Dynamics and Earthquake Engineering
M. Papadrakakis, V. Papadopoulos, V. Plevris (eds.)
Crete Island, Greece, 25–27 May 2015

EVALUATION OF THE STIFFNESS AND DAMPING OF ABUTMENTS TO EXTEND DIRECT DISPLACEMENT-BASED DESIGN TO THE DESIGN OF INTEGRAL BRIDGES

Stergios A Mitoulis[1], Sotiris Argyroudis[2], and Mervyn Kowalsky[3]

[1] Department of Civil and Environmental Engineering
University of Surrey, UK
s.mitoulis@surrey.ac.uk

[2] Department of Civil Engineering
Aristotle University of Thessaloniki, Greece
sarg@civil.auth.gr

[3] Department of Civil, Construction & Environmental Engineering
North Carolina State University, USA
kowalsky@ncsu.edu

Keywords: integral, abutment, bridge, backfill, interaction, damping.

Abstract. *There is an urgent need for maintenance-free transportation infrastructures worldwide. Integral Abutment Bridges (IABs) are robust structures, without bearings or expansion joints that require zero or minimum maintenance. The challenge to the assessment of existing and the application of IABs is the dynamic interaction between the bridge and the backfill soil. In many cases, this interaction is misinterpreted due to the inherent non-linear behavior of the soil during the so-called in-service interaction, which modifies drastically the stresses within the backfill soil under daily displacements of the abutment. A step towards the better understanding of the seismic response of IABs is the evaluation of the resistance of the abutment, which depends upon the geometry of the abutment, the properties of the soil and the successive interactions, i.e. quasi-static, under thermal expansion and contraction of the deck, or dynamic, when the bridge is subjected to seismic excitations and/or breaking loads. Towards this end, this paper attempts to: (a) interpret the condition of the abutment and the backfill soil at the onset of the dynamic excitation based upon the antecedent in-service interaction of the components and (b) to evaluate the stiffness and the damping properties of existing and/or representative integral abutments under dynamic loads to extend the Direct Displacement-Based Design (DDBD) to the design of integral bridges. A typical geometry of the integral abutment and typical backfill soil is investigated based on 2D fully coupled FE simulations adopting a visco-elasto-plastic stress model for the soil (coupled approach) under static and dynamic loads.*

1 INTRODUCTION

Integral Abutment Bridges (IABs) are structures that require minimum or zero maintenance. The barrier for the extended application of IABs is the limited knowledge on the bridge-backfill interaction, namely the in-service displacements of the deck, the consequent movements of the abutment and its non-linear interaction with the backfill soil [1] [2] [3]. On the other hand, there is an acknowledged lack of codes to provide guidance for the design of IABs, as the only standards that support their design are BA 42/96 [4] and BD 37/01 [5], which in principle require that all bridges with a length of less than 60 metres should be integral. More importantly, for earthquake resistant bridges, the use of integral abutments requires the use of a behaviour factor [6] equal to 1 and 1.5 when the bridge is locked in backfills and for abutments rigidly connected to the deck respectively. The aforementioned problems are more challenging in longer bridges, due to the fact that large daily and seasonal movements of the abutment [7] are imposed on the backfill soil. This interaction adversely affects both the long term response of the structure and the condition of the backfill soil, as it imposes settlements and permanent dislocations of the abutment.

It has been recognised that the backfill soil is a source of stiffness [8] [9] [10] and damping due to the highly non-linear response of the soil [11] [12]. This has been addressed by past studies [1] [13] [14] [15] and Caltrans seismic design criteria [8] (section 2.1.5). Despite the large number of numerical and experimental studies on the stiffness of integral abutments there are not many studies available for the estimation of the damping, which influences mainly the displacements of the bridge, but not the overall dynamic response [15]. The design and assessment of integral bridges by the displacement-based design method requires the control of the inelastic lateral displacements. One such method is the Direct Displacement-Based Design (DDBD) approach [14] that utilises the concept of equivalent linearisation to predict the response of inelastic systems with equivalent linear properties of effective stiffness and equivalent viscous damping. Several studies have been conducted to verify the performance of this method for a variety of bridges [16] [17] [18]. However, integral bridges are structures of short fundamental periods, which are expected to remain elastic under the design earthquake, whilst the effective stiffness of the bridge that is strongly dependent on the stiffness of the backfill soil, is required for the equivalent linearisation of the system. Additionally, the yielding of the backfill soil material under the seismic displacements of the deck requires a reliable estimation of the damping ratio to estimate the displacement of the equivalent linear system. Towards this end, bridge systems with fundamental periods ranging from 0.4 to 0.8 sec were analysed. The bridges had a typical integral abutment and backfill soil. Numerical analyses of the coupled abutment-backfill system were performed with the FE code PLAXIS adopting a visco-elasto-plastic stress model for the soil and the equivalent damping ratios were estimated based on the derived force-displacement curves. Subsequently, the concept of equivalent viscous damping that was first proposed by Jacobsen [19] to approximate the steady forced vibration response of linear SDOF damped systems was employed. The results showed that damping is successfully predicted by the proposed method for long-period systems, whilst for short period systems the method seems to underestimate the damping. Also, the method is not able to account for the formation of the voids that are developed between the abutment and the backfill soil, which reduces the stiffness of the system abutment-backfill and hence leads to larger displacements. This effect is described herein as period shift effect.

2 METHODOLOGY FOR DEVELOPMENT OF EQUIVALENT VISCOUS DAMPING MODEL FOR INTEGRAL BRIDGES

The following procedure was applied for the estimation of the equivalent viscous damping model for integral bridges. The successful prediction of the equivalent damping was assessed with three bridge cases having periods ranging from 0.4 to 0.8 sec.

Step 1 Generation of time histories and average compatible design spectrum.

Seven artificial accelerograms compatible to EC8-1 spectrum for soil C and PGA=0.5g were generated with Seismoartif [20] for damping ratios ranging from 5% to 35%. Subsequently, the average displacement response spectra were generated. Figure 1 shows the acceleration response spectra of the artificial accelerograms, the average spectrum of the artificial motions (red line) and the type 1 response spectrum of EC8-1 (blue line) for 5 percent damping.

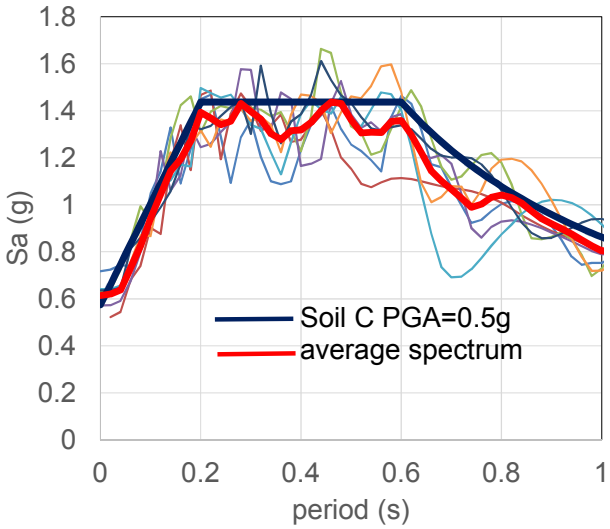

Figure 1: The acceleration response spectra of the artificial accelerograms and the average spectrum (red) and the EC8-1 type 1spectrum for Soil C and PGA=0.5g (blue).

Also, Figures 2a and 2b show the displacement response spectra of the artificial accelerograms, the average spectrum of the artificial motions (red line) and the response spectrum of EC8-1 (blue line) for 5% damping. Small discrepancies are observed in the range of periods between 0.6 and 0.8 sec. The average values of the design spectrum for these seven compatible accelerograms at the corresponding seven values of damping are then obtained, which represent average compatible design spectra for 5% to 35%, Figure 3.

Step 2. **Determination of design displacement demand**

Step 2.1 Hysteretic damping of the abutment-backfill

The effective period is selected and the equivalent viscous damping (ξ_{eq}) is estimated (eq. 1). The simplest approach for estimation of hysteretic damping is proposed by Jacobsen [19], as given by eq. 2, where A_{1oop} is the area of the hysteretic loop and A_{RPP} is the area of the rigid-perfectly plastic rectangle that encloses the loop. Figure 5d shows the graphical representation of the parameters.

$$\xi_{eq}=\xi_{el}+\xi_{hyst} \quad (1)$$

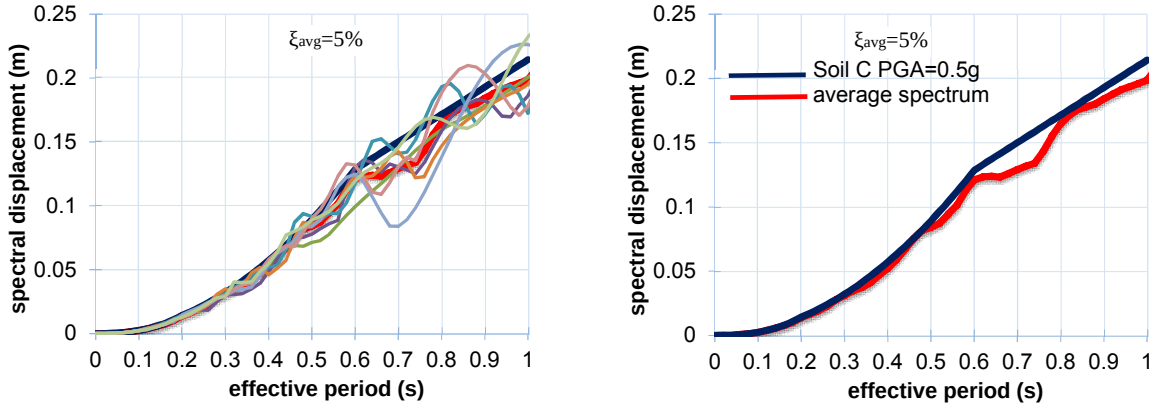

(a) (b)

Figure 2: (a) The displacement response spectra of the artificial accelerograms and the average spectrum (red); (b) comparison of the average response spectrum of the artificial motion (red) with the EC8-1 displacement spectrum (blue) for ζ_{avg}=5%, Soil type C and PGA 0.5g.

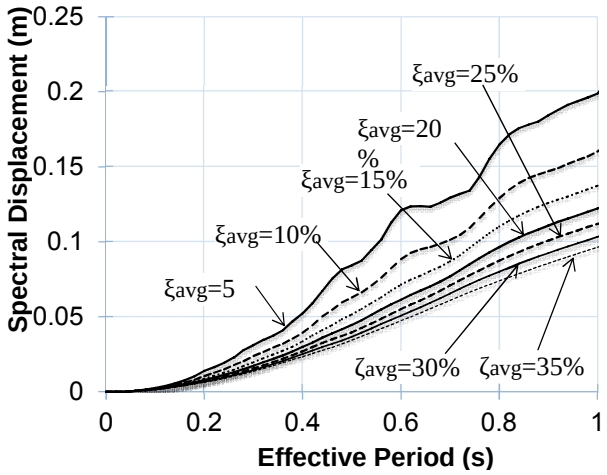

Figure 3: Average displacement response spectra for ξ_{avg} ranging from 5 % to 35 %.

In eq. 1, ξ_{el} corresponds to the damping in the elastic range and ξ_{hyst} corresponds to the damping due to energy dissipation in the abutment-backfill system. Damping in the elastic range is used to represent the damping that is not captured by the hysteretic model adopted for the analysis such as energy dissipation due to nonlinearity in the elastic response. Traditionally, this term is taken as 5 % of critical damping for reinforced concrete structures.

$$\P_{hyst} = \frac{2}{\circledR} \cdot \frac{A_{loop}}{A_{RPP}} \quad (2)$$

For the estimation of the hysteretic damping ratio ξ_{hyst}, two different loading conditions were considered, as shown in Figure 4, for the system abutment-backfill. It was found that the system abutment-backfill has different stiffness and damping when loading 1 or 2 was applied on it. More specifically, it was found that the abutment has greater stiffness and smaller damping when the abutment initially pushes the backfill and subsequently moves away from it (loading 1, shown in Figure 4a). The opposite was found to be valid, i.e. smaller stiffness and higher damping, when the abutment first moves away from the backfill and then pushes the backfill (loading 2), as shown in Figure 4b. This is also given in Table 1.

Subsequently the F-d curves of the bridge-abutment-backfill system were obtained for short period integral bridges. Analysis of bridge-abutment-backfill systems with fundamental periods 0.4 to 0.8 sec was performed. The input motion was a sinusoidal input motion with periods ranging from 0.4 to 0.8 sec. As an example, Figure 6 shows the two loadings that were employed to excite the short period system that had a fundamental period of 0.4 sec. The input motions in Figure 6 are not symmetrical due to the different stiffnesses of the abutment under loading conditions 1 and 2. Target displacements (d_t) in the range of 25mm to 130 mm were obtained for one full cycle of loading.

It is noted that Figure 5 shows the F-d response of the overall bridge system that took into account the equivalent stiffness at maximum displacement of one abutment under loading 1 (K_{ps}), one abutment under loading 2 (K_{pl}) and the stiffness of the bridge (K_b) i.e. the stiffness of the bridge piers. This is further explained in step 2 below and by equation 3. Also, Table 2 summarises the K_{ps} and K_{pl} values for different bridge systems that were analysed. The values of the ξ_{eq} given in Table 1 correspond to the sum of the elastic damping ratio plus the average damping ratio of the two loading conditions (cond. 1 and 2), because when one abutment is pushing the backfill soil, the other one is moving away from the relevant backfill soil.

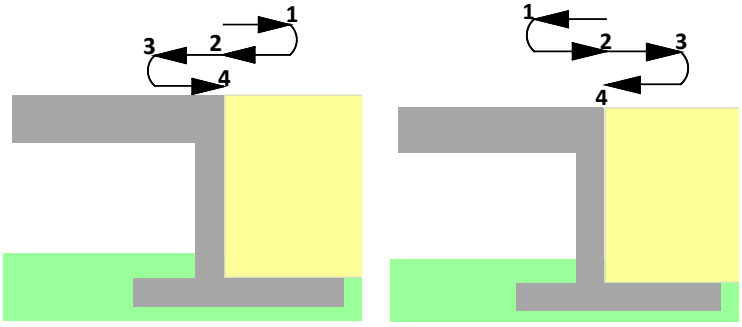

(a) push-pull (b) pull-push

Figure 4. (a) loading 1: the abutment first pushes (ps) the backfill soil and (b) loading 2, the abutment first pulls (pl) the backfill soil.

bridge period (sec) **target displ. d_t (mm)**	**ξ_{el} (%)**	**$\xi_{hyst,1}$ (%)** loading 1: push	**$\xi_{hyst,2}$ (%)** loading 2: pull	**ξ_{eq} (%)** ξ_{el}+aver($\xi_{hyst,1}$+$\xi_{hyst,2}$)
0.4 sec 25 mm	5%	11.3%	14.8%	18%
0.62 sec 60 mm	5%	12%	15%	18.5%
0.8 sec 130 mm	5%	8.0%	9.8%	13.9%

Table 1: Calculation of ξ_{eq} for short period integral bridges.

bridge period (sec)/(d_t)	**K_{ps}** (kN/m)	**K_{pl}** (kN/m)
0.4 sec / (25mm)	75829.8	30716.5
0.62 sec / (60mm)	56587.4	21193.3
0.8 sec / (130mm)	32224.5	10901.3

Table 2: The stiffness of the abutment-backfill for different effective periods and target displacements ranging from 25 to 130 mm.

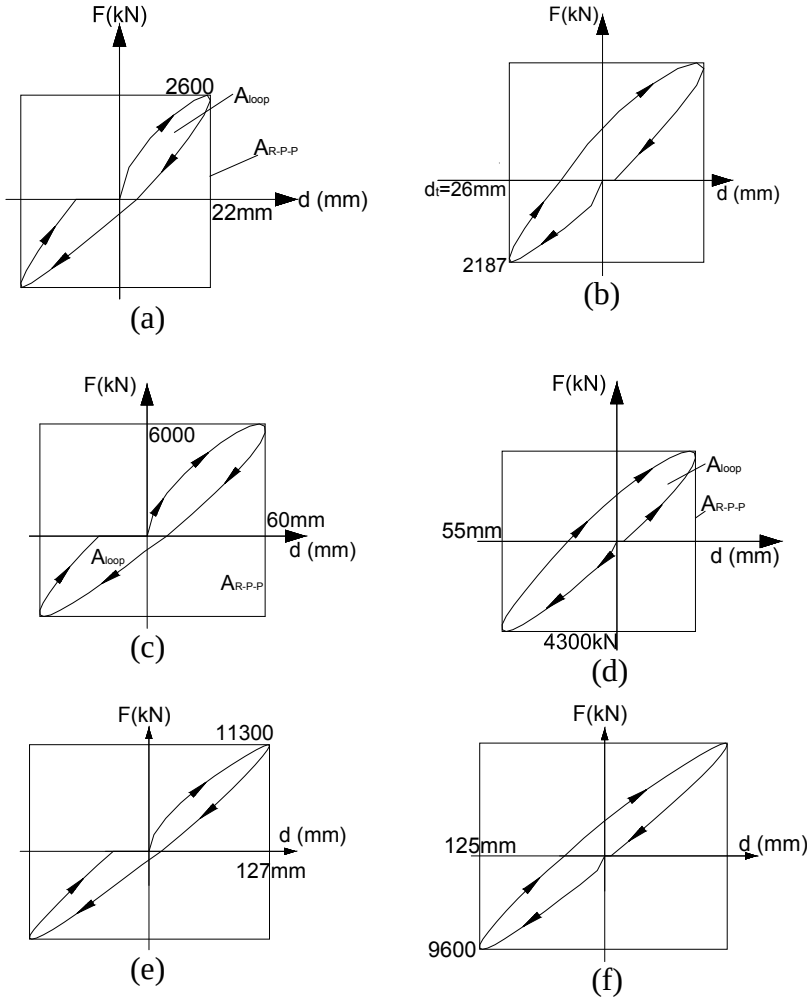

Figure 5: The F-d curves for loading condition 1: (a), (c), (e) and for loading condition 2: (b), (d), (f). Figures (a) and (b) are for T_{eff}=0.4sec and d_t=25mm, figures (c) and (d) are for T_{eff}=0.62sec and d_t=60mm and figures (e) and (f) are for T_{eff}=0.8sec and d_t=130mm (see Table 1).

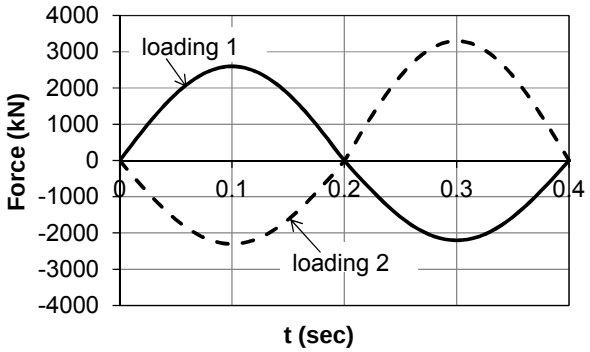

Figure 6: The input motion at the abutment for the systems with effective period 0.4 sec.

For the first iteration the equivalent viscous damping is estimated using the damping Eq. (2) for ξ_{hyst}=10%. The design displacement demand (d_t) is obtained by entering the average design spectra with the effective period (T_{eff}) to the point of the estimated equivalent viscous damping value as shown in Figure 3. Linear interpolation is used to find the damping value if it lies between two damping values of the average design spectra.

Step 3: Determination of SDOF system properties

For the analysis of the SDOF there are three components that define the stiffness, (see eq. 3), and the damping of the system, namely: (a) the bridge, which was considered to respond in an elastic manner with stiffness K_b and mass m_b, (b) the abutment that pushes the backfill soil and has an effective stiffness K_{ps} that corresponds to the target displacement d_t and (c) the other abutment that moves away from the backfill soil that has a smaller effective stiffness of K_{pl}, due to the fact that the backfill soil resists to the movement of the abutment mainly due to its self-weight that sits on the surface foundation of the abutment. Hence, the effective stiffness of the bridge-abutment-backfill system is:

$$K_{eff}=K_b+K_{ps}+K_{pl} \tag{3}$$

whilst eq. 4 relates the effective stiffness of the bridge, the mass of the bridge and the effective period of the equivalent SDOF system:

$$K_{eff}=\left(\frac{2®}{T_{eff}}\right)^2 m_b \tag{4}$$

Step 4 Characterisation of SDOF systems for nonlinear time history analysis (NLTH) of the SDOF-Determination of the Δ_{NL}.

NLTH analysis is performed to a SDOF that has ξ_{el}=5%, stiffness K_b and mass m_b, which correspond to the stiffness and mass of an integral bridge. No yielding of the structural components of the bridge was taken into account, i.e. the bridge remains elastic. The only non-linearity that was taken into account here was due to the elasto-plastic behaviour of the backfill soil. The mass of the backfill soil was not considered in m_b. The equivalent linear SDOF is given in Figure 7a. The SDOF that accounted for the non-linearities of the soil is given in Figure 7b. The SDOF is in series connected to four non-linear links that represent the non-linear response of the abutments as shown in Figure 7b. Two links that receive only compression and represent the cases where the abutment is pushing the backfill soil and two links that receive only tension and correspond to the case that the abutment is moving away from the backfill soil. The F_{ps}-d and F_{pl}-d curves were obtained by PLAXIS under two different conditions that were either push (ps) or pull (pl) of the backfill soil. For the modal analysis half of the K_{ps}^{eff} and K_{pl}^{eff} values were used as these springs in fact receive only compression or tension. The stiffnesses K_{ps}^{eff} and K_{pl}^{eff} were estimated at the target displacement that is given in Table 1, for periods of the systems ranging from 0.4 to 0.8 sec. The resulting displacements of the NLTH were averaged and the displacement Δ_{NL} was compared to the Δ_{el} (i.e. the one we obtain from Figure 3).

The F_{ps}-d F_{pl}-d curves were produced based on the bi-linearisation shown in Figure 8a. The dashed line shows the response of the system abutment-backfill soil for the push and pull conditions as calculated with the FEA in PLAXIS that is described below. The solid lines show the bi-linear curve that was used to model the non-linear response of the backfill soil. Figure 8a also shows the secant stiffness of the system abutment-backfill under loading condition 1. Figure 8b shows the response of the equivalent SDOF system of Figure 7b when the response of abutment-backfill was idealised as per Figure 8a. Figure 8b corresponds to a target displacement d_t=60mm. Similar bilinear models were used for the smaller 25 mm and larger 130mm target displacements. The figure shows that there is a reasonable agreement

between the predicted and the actual response of the system abutment-backfill for both loading conditions, i.e. push and pull. Also, Figures 8a and 8b show that indeed the system abutment has different stiffness and prospected damping for the two different loading conditions.

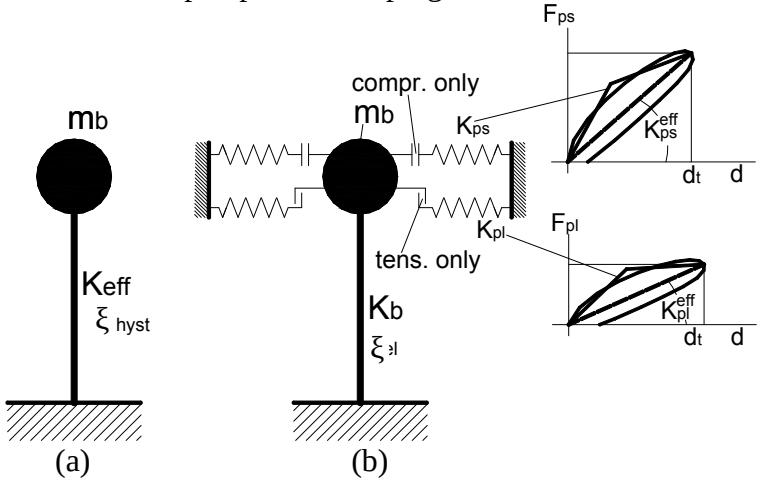

Figure 7: (a) The equivalent linear SDOF and (b) SDOF bridge model employed for the non-linear analysis.

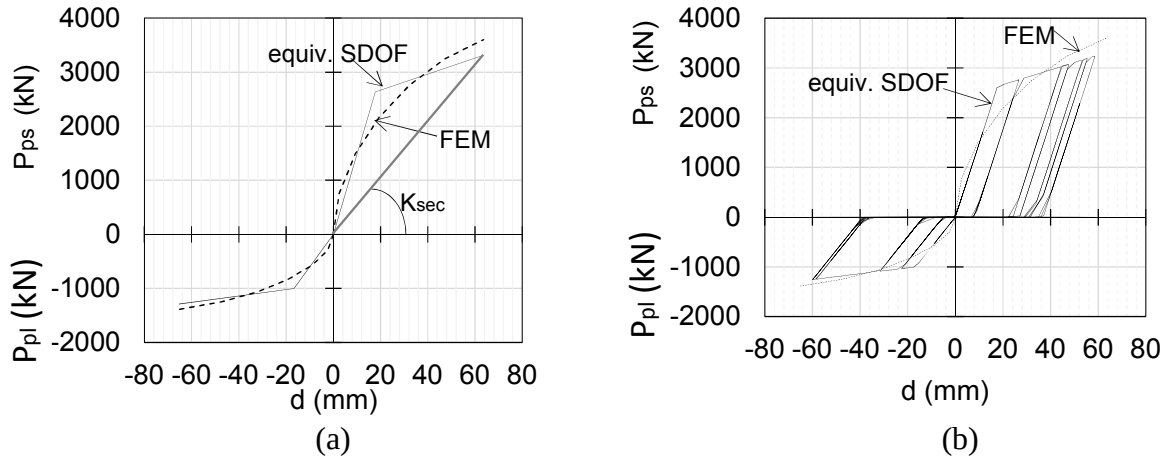

Figure 8: (a) Bi-linearisation of the F-d at target displacement (for d_t=60mm) for push (ps) and pull (pl) loading conditions 1 and 2 and (b) comparison of the F-d response bilinear curve to the response of the non-linear SDOF system.

3 MODELLING OF ABUTMENT-BACKFILL SYSTEM IN PLAXIS

The coupled integral abutment-backfill interaction analyses were performed with the 2D (plane strain) finite element code PLAXIS v8.2 [21] as shown in Figure 7 The basis was assumed to be rigid and the lateral sides were characterized by standard earthquake boundaries. The total width of the model is 250m, which is sufficient to avoid boundary effects. The domain was discretised in a total of 2682 15-node plain strain triangular elements. In the area around the abutment the mesh was refined (Figure 9). The foundation soil domain was modeled with 10 horizontal layers to account for the variable stiffness with depth. In particular, a clay material is used with shear wave velocity (V_s) that varies from 180 m/s at the surface to 310 m/s at the bottom layer, corresponding to soil type C according to the Eurocode 8. The backfill was modeled in 17 horizontal layers. A sandy material with an average V_s equal to 270m/s was selected for the backfill. The values of other soil properties were consistently selected. The integral connection of the abutment to the bridge deck is modeled through a rotation fixity and a fixed-end anchor at the top of the abutment. The axial stiffness of the anchor

has been estimated equal to E·A/L where E·A=2.637·10^7 kN/m for 1.0m of the abutment width and L is 240.0m the length of the bridge.

Initial stage analysis was performed to simulate the initial geostatic stresses. Then the dynamic analyses followed where the sinusoidal force with specific fundamental periods as described in Step 2.2 is applied at the top of the abutment. The analyses were characterised by the assumption of elasto-plastic behavior (i.e. Mohr-Coulomb criterion) for the soil and elastic behavior for the concrete elements. Proper interface elements with a friction coefficient of R_{inter}=0.70 were used to model the interface between the backfill and foundation soil with the abutment [11].

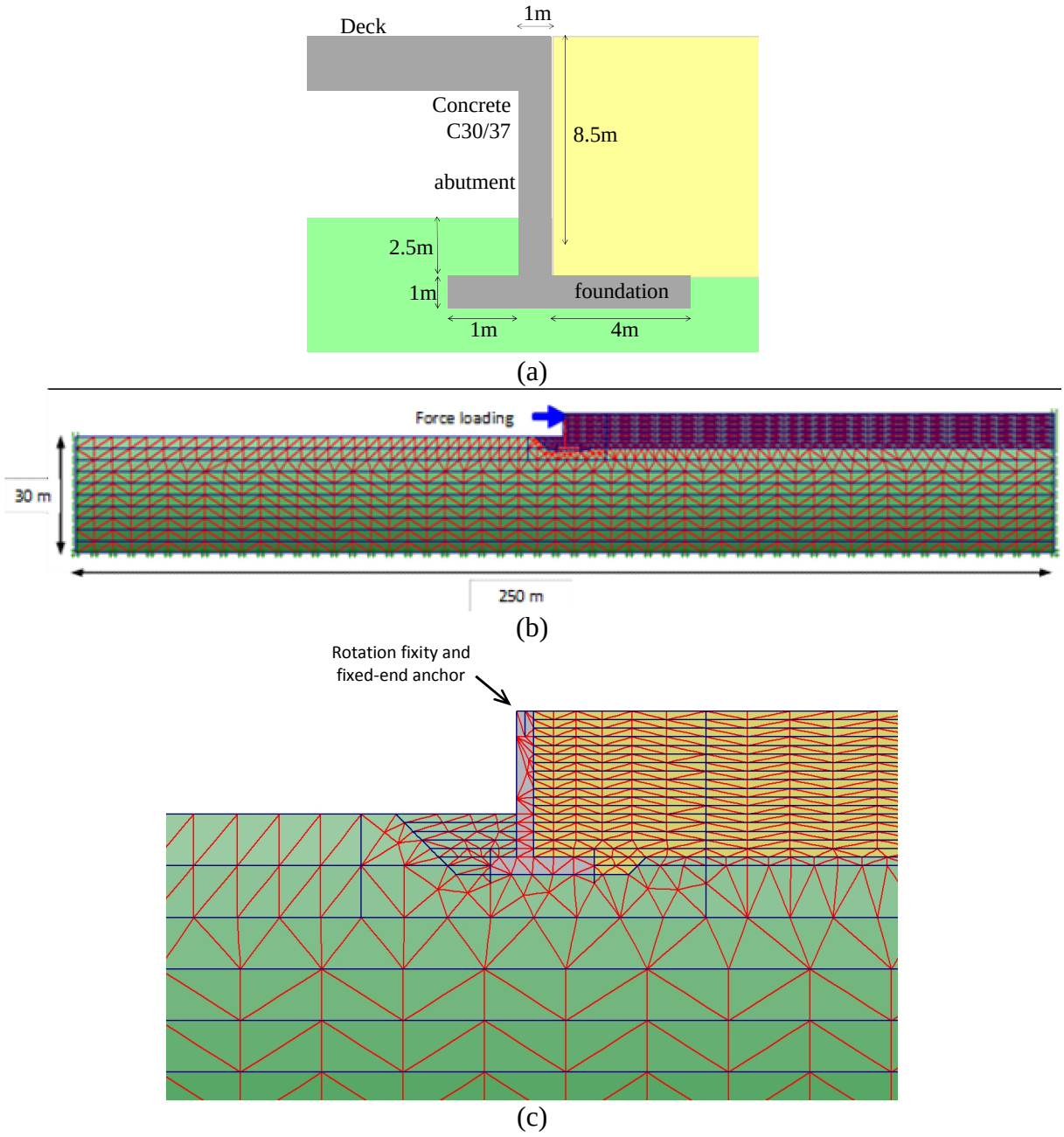

Figure 9: (a) The geometry of the typical abutment, (b) the model of the integral abutment with the backfill soil, (c) detail of the modelling in the vicinity of the integral abutment.

4 RESULTS

The results obtained and the discrepancies of Δ_{el} and Δ_{NL} are given in Table 3.

bridge period (sec)/(d_t)	**Δ_{el}** (mm)	**Δ_{NL}** (mm)	**Δ_{el}/Δ_{NL}**
0.4 sec / (25mm)	31.4	24.5	1.28
0.62 sec / (60mm)	71.6	80.9	0.89
0.8 sec / (130mm)	114.0	115.0	0.99

Table 3: Comparison of Δ_{el} and Δ_{NL}.

For the short period bridge system that has a period of 0.4 sec it seems that the proposed procedure underestimates the hysteretic damping, which was found to be equal to 13%, according to the hysteretic damping that is proposed by Jacobsen. If Δ_{NL} is considered to be the accurate displacement of 24.6mm, this displacement corresponds to an equivalent damping ratio of approximately ξ_{eq}=30%, based on the response of the equivalent linear SDOF system, given in Figure 3. It was also found that the permanent displacement of the abutment, for a target displacement of 25 mm, was of the order of 1 mm (i.e. 4% of the d_t) for loading condition 1 and 0.8 mm for loading 2. Therefore, no considerable permanent deformation of the backfill soil is expected and hence the change in the stiffness of the system during the seismic motion due to the creation of voids between the abutment and the backfill soil is negligible.

For bridge systems with a period of 0.6 sec and a target displacement of 60mm the NLTH showed that the displacement was underestimated by the equivalent linear SDOF and hence the hysteretic damping ratio, which was found to be 12-15%, was overestimated. However, the non-linear response of the backfill soil results in the formation of clearances behind the abutment, i.e. gap are formed between the abutment and the backfill soil during the dynamic response of the system. The magnitude of this gap increases during the seismic displacements of the abutment, as it is becoming larger gradually when the abutment pushes the backfill soil and the latter yields, and also when the abutment moves away from the backfill soil. Hence, the stiffness of the system abutment-backfill soil decreases along the earthquake motion and this is described here as period shift effect. This effect is important as the increase in the period was found to be of the order of 18% for the bridge that has an effective period of 0.6 sec. The permanent displacement of the abutment top, for a target displacement of 60 mm, was 14 mm (i.e. 25% of the d_t) for loading 1 and 10 mm for loading 2. This has also been described by Dwairi [16] as softening effect. One way to account for this effect is to use the secant stiffness at maximum deformation, which will account for the formation of the gaps as per Kowalsky et al. [22]. Hence, it is believed that the non-linear displacements Δ_{NL} are larger than the elastic ones Δ_{el} due to the fact that gaps are being formed behind the abutment.

For the bridge system with a period of 0.8 sec, it seems that equivalent damping ratio is predicted successfully as the equivalent elastic system and the non-linear analysis of the SDOF yielded approximately the same displacements. In this case, the absolute permanent displacement of the abutment top for the target displacement of 130mm, was 57 mm for loading 1 and 61 mm for loading 2.

Also, Figure 10 shows the areas of the backfill soil that exhibited plastic deformations when the abutment displacement was 20, 60 and 80 mm. The Figure suggests that the permanent dislocations (displacement and rotation) of the abutment is very small when the displacements are 20mm and hence no significant permanent displacement of the abutment is observed. On the contrary, when the displacement of the abutment is 60 or 80mm both the foundation of the abutment and the backfill soil yields and as a result the abutment exhibits significant permanent, dislocations which is in line with the above findings.

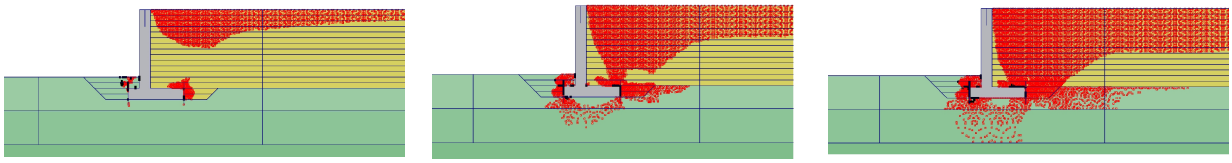

(a) (b) (c)

Figure 10: Points in the backfill soil where plastic deformation of the soil material is developed for 20, 60 and 80 mm.

5 CONCLUSIONS

The response of short period systems was studied for integral abutment bridges. The aim of the research was to define the stiffness and the equivalent damping ratio of the system bridge-abutment-backfill to extend the use of DDBD method to existing and new IABs. FEM software PLAXIS was used to obtain the force-displacement curves of the system abutment-backfill under dynamic loads having fundamental periods ranging from 0.4 sec to 0.8 sec. Non-linear response of the system was considered due to both the material non-linearities (soil) and due to the development of voids between the abutment and the backfill soil. The equivalent damping ratio of the integral bridge system (bridge-abutment-backfills) accounted for the elastic damping (ξ_{el} =5%) and the hysteretic damping (ξ_{hyst}) due to the inelastic behaviour of the backfill soil. The damping model did not take into account the mass of the backfill soil or other types of damping. The results showed that for the bridge systems with periods in the range of 0.6 to 0.8 sec the equivalent damping ratio can be predicted with adequate accuracy by the proposed methodology. For the short period systems the methodology was found to underestimate the damping ratio and hence overestimate the displacement by 28%.

It was evident throughout the analyses of different bridge systems that the hysteretic damping of the system abutment-backfill was not strongly dependent on the magnitude of the target displacement, as for greater target displacements the damping ratio, was not increased significantly. On the contrary, greater frequencies of the input motion lead to larger damping ratios. The equivalent damping ratios for bridge systems having periods in the range of 0.4 – 0.8 sec was found to be in the range of 14-18.5%.

The softening of the system due to the yielding of the backfill soil, the gaps that are formed between the abutment and the backfill soil during an earthquake and the significantly different response of the abutment when it pushes the backfill soil and when it moves away from it, complicate the interaction problem. The above, along with the geometry of the abutment, the foundation soil and the properties of the backfill soil will be the object of further investigation.

REFERENCES

[1] J. Lu, A. Elgamal, K. Mackie, A. Shamsabadi, A framework for performance-based earthquake engineering of bridge-abutment systems. RD. Hyrciw, A. Athanasopoulos-Zekkos, N. Yesiller eds *Geo-Congress 2012: State of the Art and Practice in Geotechnical Engineering*, Geotechnical Special Publication No.225, ASCE Geo-Institute, March 25-29, 2012.

[2] S. Mitoulis, Seismic design of bridges with the participation of seat-type abutments, *Engineering Structures*, **44**, 222-233, 2012.

[3] S. Mitoulis, S. Argyroudis, K. Pitilakis, Green rubberised compressible inclusions to enhance the longevity of integral abutment bridges. *2nd European Conference on Earthquake Engineering and Seismology*, Istanbul, Turkey, 25-29 August, 2014.

[4] BA 42/96, The design of integral bridges, *Highways Agency*, UK, 2003.

[5] BD 37/01, Design manual for roads and bridge, *Highways Agency*, UK, 2001.

[6] EN 1998-2, Eurocode 8: Design of structures for earthquake resistance, Part 2: Bridges, 2005.

[7] A. Lemnitzer, E. Ahlberg, R. Nigbor, A. Shamsabadi, J. Wallace, J. Stewart, Lateral perfor-mance of full-scale bridge abutment wall with granular backfill, *Journal of Geotechnical and Geoenvironmental Engineering*, **135**, 506-514, 2009.

[8] California Department of Transportation (CalTrans), Seismic design criteria, Version 1.7, April, 2013.

[9] O. Taskari, A. Sextos, Probabilistic assessment of abutment-embankment stiffness and implications in the predicted performance of short bridges, *Journal of Earthquake Engineering*, doi:10.1080/13632469.2015.1009586, 2015.

[10] P. Wilson, A. Elgamal, Large-scale passive earth pressure load-displacement tests and numerical simulation, *Journal of Geotechnical and Geoenvironmental Engineering*, **136,** 1634-1643, 2010.

[11] S. Argyroudis, AM. Kaynia, K. Pitilakis, Development of fragility functions for geotechnical constructions: Application to cantilever retaining walls, *Soil Dynamics and Earthquake Engineering*, **50**, 106-116, 2013.

[12] A. Shamsabadi, P. Khalili-Tehrani, J. Stewart, E. Taciroglu, Validated simulation models for lateral response of bridge abutments with typical backfills, *Journal of Bridge Engineering*, **15,** 302-311, 2010.

[13] A. Shamsabadi, S-Y. Xu, E. Taciroglu, A generalized log-spiral-Rankine limit equilibrium model for seismic earth pressure analysis, *Soil Dynamics and Earthquake Engineering*, **49**, 197-209, 2013.

[14] MJN. Priestley, GM. Calvi, MJ. Kowalsky, *Direct displacement-based design of structures*. IUSS Press, Pavia, Italy, 2007.

[15] J. Wilson, B. Tan, Bridge abutments: assessing their influence on earthquake response of Meloland road overpass, *Journal of Engineering Mechanics*, **116**, 1838-1856, 1990.

[16] H. Dwairi, M. Kowalsky, J. Nau, Equivalent damping in support of direct displacement-based design, *Journal of Earthquake Engineering*, **11**, 512-530, 2007.

[17] E. Khan, TJ. Sullivan, MJ. Kowalsky, Direct displacement–based seismic design of reinforced concrete arch bridges, *Journal of Bridge Engineering*, **19**, 44-58, 2014.

[18] W. Kwan, S. Billington, Influence of hysteretic behavior on equivalent period and damping of structural systems, *Journal of Structural Engineering*, **129**, 576-585, 2003.

[19] LS. Jacobsen, Steady forced vibrations as influenced by damping. *Transactions of the American Society of Mechanical Engineers*, **52**, 169-181, 1930.

[20] SeismoSoft. Earthquake Engineering Software Solutions. Seismoartif, ver. 2.1.0, 2015.

[21] Plaxis 2D, *Reference Manual*, Version 8, 2008.

[22] MJ. Kowalsky, MJN. Priestley, GA. MacRae, Displacement-based design of RC bridge columns in seismic regions, *Earthquake Engineering and Structural Dynamics*, **24,** 1623-1643, 1995.